

THE EMPLACEMENT AGE OF GABBROIC ROCKS AND ASSOCIATED GRANITOIDS OF THE LIGANGA MSANYO COMPLEX, SOUTH EASTERN TANZANIA

MAH Maboko

Department of Geology, University of Dar es Salaam
P.O. Box 35052, Dar es Salaam, Tanzania

ABSTRACT

The Msanyo Gabbro and the associated Mdando granitoids, which intrude Paleoproterozoic high-grade metamorphic rocks of the Ubendian Belt in southern Tanzania, yield imprecise Sm-Nd whole rock isochron ages of 1608 ± 134 Ma ($\epsilon(\text{Nd}) = 2.1$) and 1642 ± 100 Ma ($\epsilon(\text{Nd}) = 1.6$), respectively. These ages are indistinguishable at the 95% confidence level, indicating that the two rock suites were intruded at the same time. A more precise estimate of the time of emplacement is provided by a 5-point mineral isochron age of 1505 ± 42 obtained from one of the gabbro samples. Calculated initial $\epsilon(\text{Nd})$ values and mean crustal residence ages are similar for both rock suites and range from -0.7 to 1.5 and 1.7 to 1.9 Ga, respectively. Initial Sr isotope ratios lie between 0.7032 and 0.7039 and these values are similar to those obtained in the mantle and the lower continental crust. The rather evolved Nd isotope systematics, combined with the relatively non-radiogenic Sr isotopic signature, suggest that both suites crystallised from mantle-derived magma that had assimilated a significant amount of lower continental crustal material. Subsequent to their emplacement, the rocks experienced localised shearing and sericitisation during the Ukingan tectonic event. A Rb-Sr plagioclase-whole rock age dates this event at 1137 ± 50 Ma.

INTRODUCTION

Isolated bodies of anorthositic to gabbroic rocks intrude the Palaeoproterozoic metamorphic rocks of the Ubendian Belt along a ~160 km front in southern Tanzania extending from central-east Upangwa to northern Ukinga (Fig. 1). Associated with these bodies are smaller granitic to syeno-granitic bodies whose field relation with the gabbroic masses is unclear. Stockley (1948) observed that the gabbroic rocks show a progressive change from anorthosite and leucogabbro in the southern and topographic lowest bodies through norite and olivine norite to ultrabasic. Parallel with this grading is a similar change from leucogabbro to quartz diorite and syeno-granite. The two differentiates lie side by side although the granitoids tend to occupy topographic highs above the gabbros (Stockley 1948). The order of crystallization in the gabbroic bodies appears to be plagioclase, olivine with some magnetite and chrome spinel, hypersthene and lastly the Fe-oxide minerals ilmenite, magnetite and chrome spinel. Massive magnetite seams occur in the most southern and topographically lowest gabbro body (the Liganga mass), while small chromite bodies are found in the ultrabasic rocks. All the mafic rocks have been saussuritized during a hydration event related to a latter Ukingan shearing event (Stockley 1948). Although there is no direct connection between the individual gabbroic masses along the entire ~160 km long front of intrusion, Stockley (1948) concluded that the bodies are most likely associated and may be even connected at depth.

Within this belt, the Liganga mass is believed to contain more than 44.5 million long tons of high grade titaniferous magnetite ore (averaging 48.8% Fe, 12.8% TiO₂ and 0.67% V₂O₅) in the form of seams enclosed between anorthositic to leucogabbroic layers (Stockley 1948). Stockley (1948) considers the magnetite to have crystallized from the same magma that formed the gabbros. Despite the obvious economic importance of these bodies, their emplacement age and, therefore, the time of mineralisation remains unknown. This paper presents new Sm-Nd and Rb-Sr isotopic data from the Msanyo Gabbro and the associated Mdando Granite which form relatively fresh satellite bodies of the main Liganga mass (Fig. 1). The data is used to constrain both the age of magnetite mineralisation and the age of the post-magmatic Ukingan shearing.

Geology of the Liganga-Msanyo area

The Liganga-Msanyo gabbros occur at the southern end of the linear belt of intrusive rocks that run parallel to Lake Nyasa. The Liganga mass is predominantly anorthositic to leucogabbroic whereas the Msanyo body is predominantly melanocratic. Lenticular masses of granitic to syeno-granitic composition are associated with both gabbroic bodies. The larger of these masses is associated with the Msanyo gabbro and is referred to as the Mdando granite (Haldemann 1961). These granitic rocks generally occupy topographically higher positions relative to the gabbros. In both cases, however, the intrusive relationship between the two rock suites is obscured by

lack of exposure. Both the intrusives and the Palaeoproterozoic Ubendian country rocks were strongly sheared during mid Proterozoic time during which arenitic to argillaceous sediments of the Ukinga Group, now metamorphosed into the greenschist facies and strongly sheared, were deposited. The emplacement of both rock suites pre-date the Ukingan deformation as evidenced by discrete shear zones that cut them locally. The only obvious petrographic effects of the Ukingan event on both the gabbroic and granitic rocks is restricted to moderate to intense sericitisation of feldspars. The Liganga rocks have been heavily altered as a result of the hydrothermal activity associated with the Ukingan event whereas the Msanyo gabbro tends to be relatively more fresh. It is for this reason that the Msanyo body was selected for the present study.

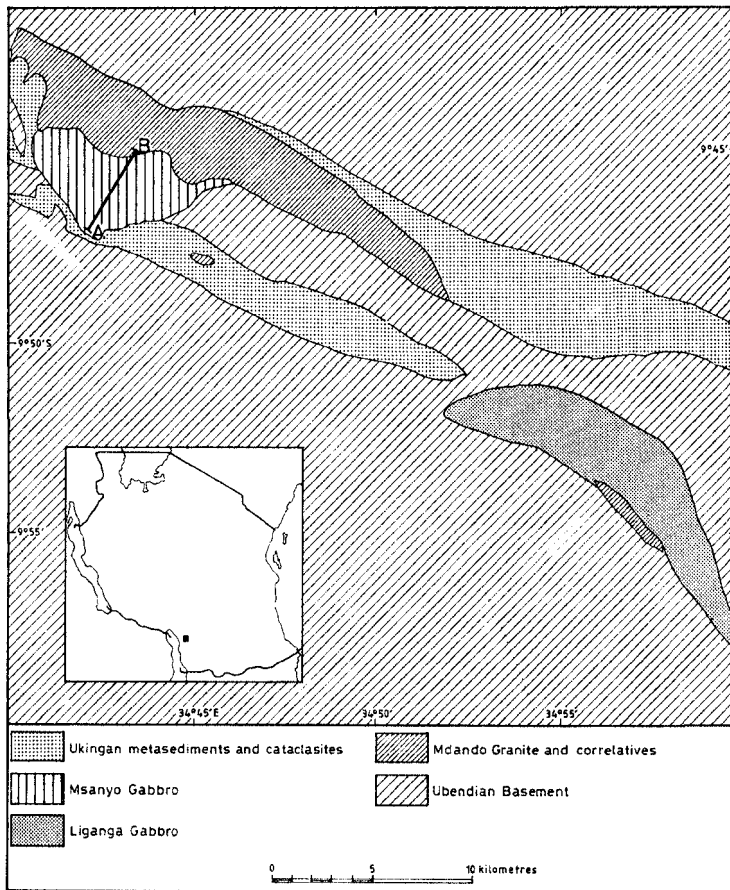


Fig 1: Geological map of the Liganga, Msanyo and Mdando complexes (After Stockley 1948). Line AB indicates the sampling traverse across the Msanyo Gabbro. The insert shows the map of Tanzania with the location of the study area indicated by the solid square

METHODS

Four gabbroic and five granitic samples collected across the Msanyo Gabbro and the southern margin of the adjoining Mdando granite were analysed for Sr and Nd isotopic composition as well as Sr, Nd, Sm and Rb concentrations at the Pheasant Memorial Laboratory (PML) for Geochemistry and Cosmochemistry of the Institute for the Study of the Earth's Interior at Misasa, Japan, using a Finnigan MAT262 mass spectrometer. The sampling sites are indicated on Fig. 1. In addition, high purity mineral separates of plagioclase, clinopyroxene (two fractions of different magnetic susceptibility) and orthopyroxene were obtained from one sample (UB19) using conventional heavy liquid and magnetic separation techniques. The mineral separates were acid leached, and similarly analysed for Sr and Nd isotopic compositions as well as Sr, Nd, Rb and Sm concentrations. The analytical procedure for chemical separation and mass spectrometry are described in Yoshikawa and Nakamura (1993) for Rb-Sr and Shibata *et al.* (1989) for Sm-Nd and are essentially similar to those described in Maboko and Nakamura (1996). The isotopic ratios were normalised to $^{87}\text{Sr}/^{86}\text{Sr} = 0.1194$ and $^{146}\text{Nd}/^{144}\text{Nd} = 0.7219$. Replicate analyses of the La Jolla Nd standard gave $^{143}\text{Nd}/^{144}\text{Nd} = 0.511920$ (13 (2σ , $n = 9$)) whereas the NBS 987 standard gave $^{87}\text{Sr}/^{86}\text{Sr} = 0.710224 \pm 8$ (2σ , $n = 8$). Maximum 2σ uncertainty in the Sm/Nd and Rb/Sr ratios derived from long term reproducibility of standard samples is 2%. Typical blank values are 5 and 10 pg for Sm and Nd respectively and negligible. Corresponding values for Rb and Sr are 25 and 35 pg respectively and equally negligible.

The major element compositions together with Ni and Cr contents of the rock samples were analysed on fused disks using a Phillips PM2400 X-ray fluorescence spectrometer. The trace element analyses were performed on a YOKOGAWA PM@2000 ICP-MS using the flow injection method (Makishima and Nakamura 1997). The analytical reproducibility is better than 6.5% and typically ~2.5% for trace elements and better than 0.2% for the major elements. Chemical compositions of the analysed minerals were performed using a Horiba EMAX-7000 energy dispersive X-ray spectrometer assembled onto a Hitachi S-3100H scanning electron microscope. Regression analysis of the isotopic data was performed using the Isoplot routine of Ludwig (1994).

RESULTS

Petrography

Sample UB14 is a pure anorthosite consisting of plagioclase which is intensely sericitised locally. Epidote may also form in the zones of extreme sericitization. UB16 is a leucogabbro consisting of fresh coarse plagioclase, clinopyroxene and orthopyroxene listed in decreasing order of abundance. Minor phases include biotite as an alteration product of orthopyroxene and

opaque Fe-Ti oxides. UB18 is a coarse-grained gabbro consisting of plagioclase, clinopyroxene and orthopyroxene as the major phases. Opaques and biotite are minor phases. The clinopyroxene partially rims orthopyroxene suggesting the crystallisation sequence orthopyroxene → clinopyroxene.

Sample UB19 is a medium-grained gabbro consisting of plagioclase ($An_{0.62}$), clinopyroxene ($En_{0.47}Wo_{0.41}Fs_{0.12}$), olivine ($Fo_{0.77}$) and orthopyroxene ($En_{0.81}$) with subordinate amounts of opaque Fe-Ti oxides. Most of the clinopyroxene grains have dirty brown surfaces caused by the exsolution of tiny inclusions of ilmenite oriented in such a way that they intersect cleavage traces at an angle of $\sim 60^\circ$. The olivine occurs as large grains cut by cracks which are filled with serpentine. The sequence of crystallisation as deduced from rimming relationships of the phases is: olivine → orthopyroxene → plagioclase → clinopyroxene.

Sample UB21 is a fine-grained dyke intruded along the margin between the gabbro and the granitic body that outcrop in the northern part of the area (Fig.1). It consists of plagioclase and clinopyroxene which has been heavily altered to, and in some cases almost completely replaced by chlorite and, to a lesser extent, biotite. The alteration of clinopyroxene is associated with the formation of opaque Fe-Ti oxides, which also constitute a major phase. Samples UB20 and UB22 are granites consisting of microcline, plagioclase and quartz as the major constituents. Green-brown biotite associated with opaque Fe-Ti oxides, hornblende and epidote are minor phases. The plagioclase is strongly sericitised whereas the quartz has been deformed as evidenced by the presence of deformation bands, sutured margins and the presence of a fine mosaic of annealed sub-grains mantling the larger quartz and feldspar grains. The main petrographic difference between UB20 and UB22 is the relatively lower abundance of quartz and biotite in the latter. Sample UB23 is a relatively mafic syeno-granite consisting predominantly of plagioclase (strongly sericitised), microcline, hornblende and a subordinate amount of quartz. The hornblende is locally altered to form a later generation bluish hornblende. The formation of opaque Fe-Ti oxides, apatite, epidote and sphene is also associated with this alteration. UB24 is a less felsic rock which is otherwise petrographically similar to UB23 except for the presence of biotite, higher abundance of quartz and less abundance of hornblende.

Geochemistry

The major and trace element composition of the Msanyo gabbros and associated Mdando granitoids is presented in Table 1. To facilitate discussion, the basic rocks with 45-50% SiO_2 are referred to as gabbros whereas the more sialic rocks with SiO_2 contents of 55-75% are referred to as granitoids. On a total alkali (Na_2O+K_2O) versus SiO_2 plot (Fig. 2) both gabbros and granitoids define a smooth trend that mimics the alkaline differentiation trend of Miyashiro (1974).

Table 1: Major (in weight%) and trace element (in ppm) compositions of the Msanyo gabbroic and granitic rocks, Tanzania

	UB14	UB16	UB18	UB19	UB21	UB20	UB22	UB23	UB24
SiO ₂	50.2	49.0	47.9	45.2	55.1	65.4	74.8	60.1	68.3
TiO ₂	0.22	0.34	0.20	0.24	1.4	0.97	0.12	0.92	0.57
Al ₂ O ₃	28.4	25.9	23.8	19.4	14.4	14.0	12.4	14.5	12.7
Fe ₂ O ₃	0.98	3.3	6.0	8.0	10.0	5.6	0.9	8.2	4.1
MnO	0.02	0.04	0.07	0.11	0.18	0.07	0.01	0.19	0.08
MgO	0.21	2.08	5.38	10.9	3.16	0.26	0.08	0.79	0.42
CaO	12.4	11.7	10.6	10.8	5.8	1.6	0.62	3.3	1.6
Na ₂ O	4.1	3.6	3.2	2.1	4.2	3.7	3.6	4.2	3.3
K ₂ O	0.52	0.44	0.41	0.17	2.5	5.1	5.0	4.8	5.1
P ₂ O ₅	0.02	0.02	0.03	0.02	0.27	0.06	0.01	0.33	0.12
Ni	5.6	85.7	233	385	42.8	3	0.50	5.6	2.9
Cr	17.0	18.0	24.0	305	80.0	0	0	0	0
Tot	97.0	96.4	97.7	97.0	97.0	96.7	97.5	97.2	96.3
Rb	6.8	4.3	4.7	3.3	74.8	125	177	136	144
Sr	591	622	671	324	253	63.8	39.8	129	81.8
Y	2.3	4.4	2.9	4.5	98.3	87.4	16.4	314	87.0
Cs	0.11	0.01	0.01	0.04	1.0	0.80	1.3	1.3	0.96
Ba	271	274	288	77	1354	783	722	1508	917
La	4.2	4.0	4.5	2.0	75.8	1.61	21.1	75.2	95.2
Ce	7.8	7.8	8.4	4.6	171	325	36.7	199	201
Pr	0.84	0.93	1.00	0.64	20.8	37.4	3.6	26.7	23.5
Nd	3.4	3.8	4.0	2.8	89.1	147	12.6	120	94.6
Sm	0.63	0.75	0.67	0.69	17.8	23.7	2.3	32.3	17.0
Eu	0.78	0.93	0.96	0.48	3.6	2.6	0.95	3.88	1.9
Gd	0.50	0.74	0.60	0.76	17.1	19.4	2.1	37.8	15.9
Tb	0.08	0.12	0.09	0.13	2.9	2.8	0.38	7.3	2.6
Dy	0.44	0.75	0.51	0.82	17.0	14.9	2.4	48.5	15.3
Ho	0.08	0.15	0.10	0.17	3.6	3.1	0.52	10.7	3.1
Er	0.19	0.36	0.26	0.43	9.2	8.1	1.6	30.1	8.0
Tm	0.03	0.06	0.04	0.06	1.4	1.2	0.26	4.8	1.2
Yb	0.19	0.40	0.27	0.45	9.2	8.2	1.9	31.9	8.3
Lu	0.02	0.05	0.04	0.06	1.3	1.2	0.28	4.6	1.2
Pb	5.5	1.4	1.5	0.74	16.5	21.3	10.4	32.4	23.5
Th	1.2	0.07	0.18	0.21	2.5	29.2	9.0	29.7	18.5
U	1.3	0.01	0.03	0.04	0.41	2.7	1.7	8.2	2.4
Zr	4.1	13.5	8.8	12.20	81.2		87.7		847
Hf	0.10	0.39	0.24	0.35	1.9	38.7	3.3	35.7	15.4
Nb	0.55	1.0	0.56	0.59	38.6	41.1	17.2	110	39.2
Ta	0.03	0.08	0.04	0.04	2.038	1.6	5.7	2.2	
Ti	1337	2056	1193	1456	8391	5784	707	5526	3404
K	4275	3669	3362	1403	20920	42670	41790	39681	42504
La/Nb	7.70	4.02	8.11	3.35	1.97	3.91	1.23	0.68	2.43
Ba/Nb	496.57	274.47	517.35	130.81	35.08	19.02	42.08	13.68	23.38

Table 1: Continued

Sr/Nd	172.90	164.45	169.40	117.61	2.84	0.44	3.15	1.08	0.87
Ce/Pb	1.42	5.50	5.64	6.23	10.38	15.24	3.52	6.15	8.54
Nb/U	0.43	80.16	19.00	15.52	94.56	15.29	10.11	13.48	16.46
Th/U	0.97	5.93	6.08	5.49	6.20	10.85	5.31	3.63	7.75
Nb/La	0.13	0.25	0.12	0.30	0.51	0.26	0.81	1.47	0.41

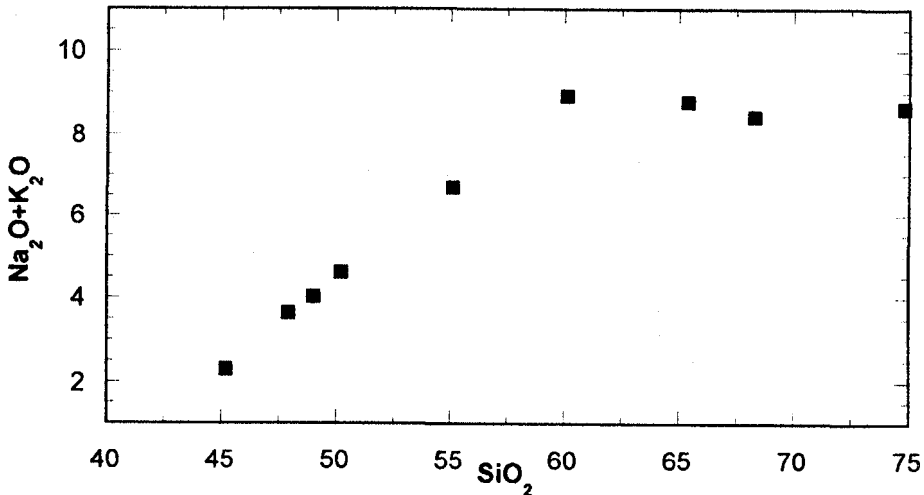


Fig. 2: Na₂O + K₂O versus SiO₂ plot for the gabbros and granitoids. Note the smooth trend suggestive of a common alkaline differentiation trend

Over all, the trace element abundances of the gabbroic rocks are lower than in the granitoids (Table 1). For example, La abundance is 6-14 times chondritic for the gabbros whereas it is 68 - 518 times chondritic for the granitic rocks (Fig. 3). Both rock suites have LREE enriched and nearly flat HREE patterns indicating melting from a relatively deep source where garnet remained as a residue phase (Brownlow 1996). The enrichment factor of the light (L) REE relative to the HREE as indicated by La_N/Yb_N ratios is similar for both compositional groups (2.93 - 14.73 and 1.59 - 13.29 for gabbros and granitoids respectively). All the gabbros have prominent positive Eu anomalies (Eu/Eu* = 2.02 - 4.64) whereas all the granitoids, except for UB22 which has a weak positive anomaly (Eu/Eu* = 1.34), have strong negative anomalies (0.33 - 0.63).

Isotopic data

Nd and Sr isotopic data together with depleted mantle mean crustal residence (T_{DM}) ages, calculated assuming a linear evolution model for the mantle and present day mantle ¹⁴³Nd/¹⁴⁴Nd and ¹⁴⁷Sm/¹⁴⁴Nd values of 0.513114 and 0.222 respectively (Michard *et al.* 1985), are shown in Table 2. The gabbros and granitoids yield similar T_{DM} ages of between 1.7 and 1.9 Ga. When

regressed together, the gabbros define an isochron corresponding to an age of 1608 ± 134 Ma (2σ error, MSWD = 2.04) and $\epsilon(\text{Nd}) = 2.1$. Corresponding values for the granitoids are 1642 ± 100 Ma (MSWD = 0.4) and $\epsilon(\text{Nd}) = 1.6$ (Fig. 4). The large errors in the isochron ages have most likely been caused by the limited spread in the Sm/Nd ratios of both suites.

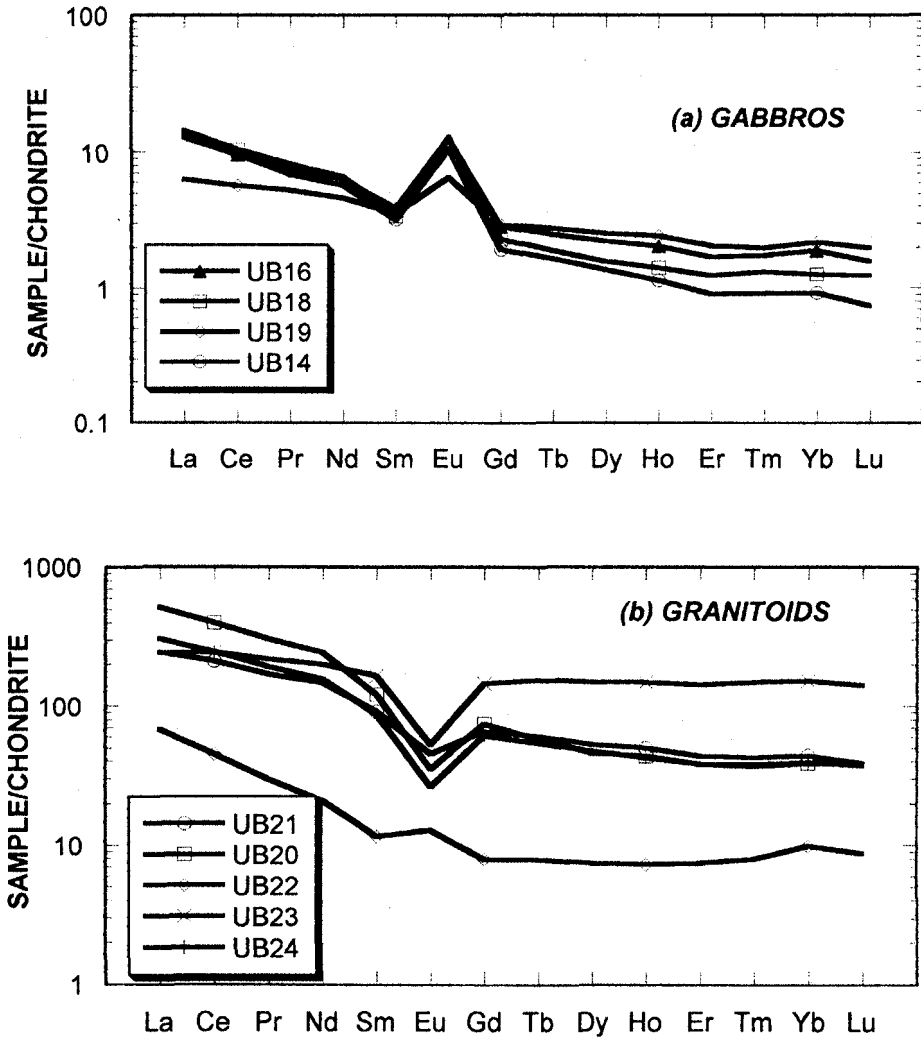


Fig. 3: Chondrite normalized REE patterns (normalizing values after Boyton 1984) for gabbros (a) and granites (b) from the Liganga-Msanyo complex, Tanzania

Table 2: Sm-Nd data

Sample	Nd (ppm)	Sm (ppm)	$^{147}\text{Sm}/^{144}\text{Nd}$	$^{143}\text{Sm}/^{144}\text{Nd}$	T*DM (Ma)	$(^{143}\text{Nd}/^{144}\text{Nd})_{1.5}$	$\epsilon(1.5)$
UB14	3.61	0.62	0.1033	0.51177±22	1712	0.51076	1.2
UB16	3.78	0.752	0.1197	0.511923±9	1770	0.51074	0.9
UB18	3.21	0.574	0.1076	0.51178±10	1770	0.51072	0.4
UB19	2.63	0.665	0.1522	0.512274±7	1828	0.51977	1.5
UB12	80.2	16.6	0.1246	0.511893±11	1904	0.51067	-0.7
UB20	188.3	29.3	0.0937	0.511599±9	1794	0.510676	-0.5
UB22	26.97	4.55	0.1015	0.511697±10	1788	0.51070	-0.1
UB23	138.2	35.7	0.1555	0.51227±14	1928	0.51074	0.7
UB24	114.6	20.8	0.1092	0.51178±11	1798	0.51070	0.1
UB19P**	2.16	0.354	0.0986	0.511731±16	1704	0.51076	1.2
UB19C1	1.11	0.429	0.2326	0.51306±19		0.51077	1.3
UB19C2	0.989	0.371	0.2258	0.513018±14		0.51079	1.8
UB19o	4.54	1.8	0.2386	0.513086±18		0.51073	0.7

*T_{DM} represents Nd depleted mantle crust formation ages (in Ma) calculated assuming a linear evolution model for the mantle together with present day mantle $^{143}\text{Nd}/^{144}\text{Nd}$ and $^{147}\text{Sm}/^{144}\text{Nd}$ values of 0.513114 and 0.222, respectively (Michard *et al.* 1985).

**P, C1, C2 and O denote plagioclase, weakly magnetic clinopyroxene, strongly magnetic clinopyroxene and orthopyroxene respectively.

Table 3: Rb-Sr data

Sample	Sr (ppm)	Rb (ppm)	$^{87}\text{Sr}/^{86}\text{Sr}$	$^{87}\text{Rb}/^{86}\text{Sr}$	$(^{87}\text{Sr}/^{86}\text{Sr})_{1.5}$
UB14	567	7.29	0.704683	8	0.7039
UB16	598	4.37	0.704261	10	0.7038
UB18	515	3.95	0.704362	7	0.7039
UB19	281	3.12	0.703900	9	0.7032
UB20	77.4	176	0.814561	8	0.6731
UB22	78.0	290	0.861396	10	0.6309
UB23	147	179	0.766964	8	0.6916
UB24	96.8	552	0.80805	8	0.4545
UB19P	435	1.75	0.703568	9	0.7033

*Initial $^{87}\text{Sr}/^{86}\text{Sr}$ ratio at 1.5 Ga.

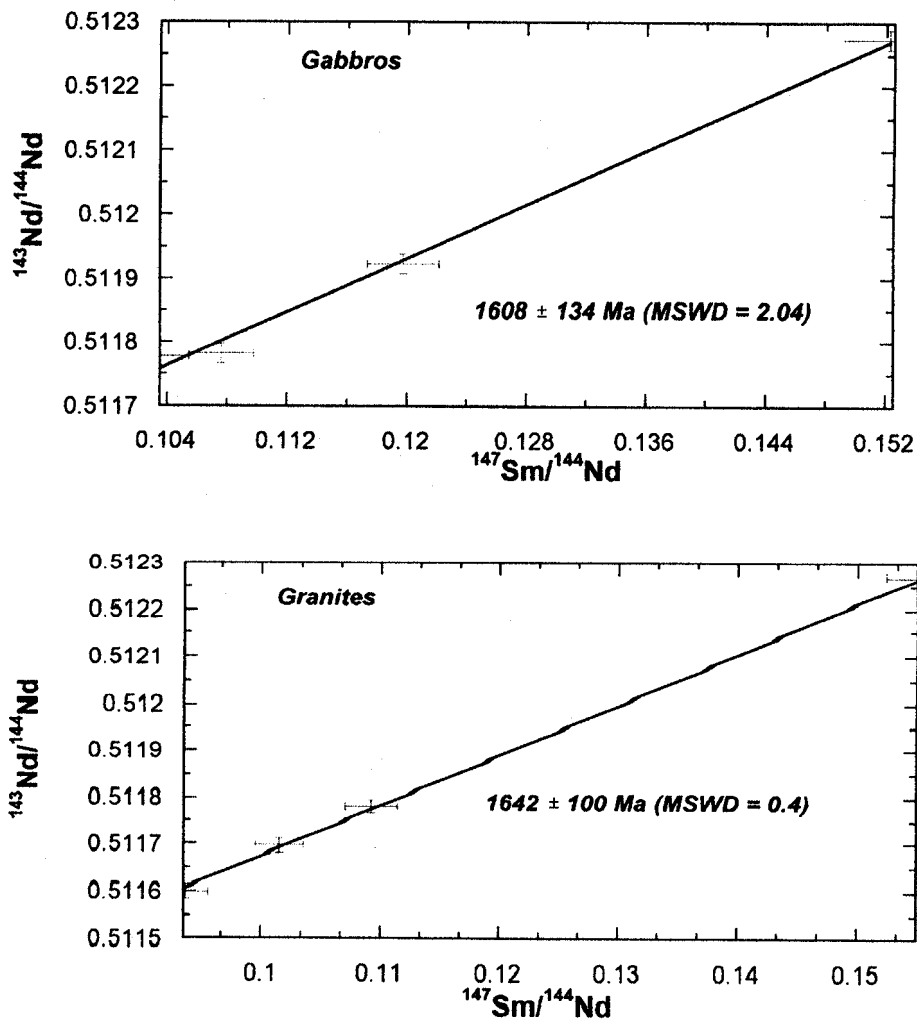


Fig. 4: Sm-Nd whole rock isochrons for gabbros (a) and granites (b) from Msanyo-Liganga, Tanzania

A better age constrain is provided by combining the isotopic data of the whole rock sample UB19 and its mineral separates (Fig. 5). The whole rock, plagioclase, two clinopyroxene fractions and orthopyroxene yield a 5 point isochron corresponding to an age of $1505 \pm 42 \text{ Ma}$ (MSWD = 1.08) and $\epsilon(\text{Nd}) = 1.3$. This age is within error of the whole rock isochron ages of both rock suites. $\epsilon(\text{Nd})$ values calculated using this age for the whole rock samples range from 0.4 to 1.5 and -0.7 to 0.7 for the gabbros and granitoids, respectively.

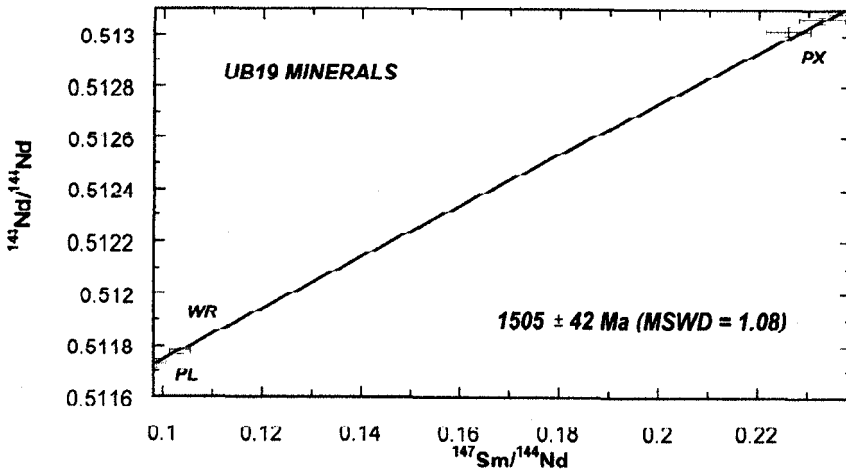


Fig. 5: Sm-Nd mineral isochron for the gabbro sample UB19, WR, PL and PX denote whole rock, plagioclase and the pyroxenes (two clinopyroxene fractions and orthopyroxene) respectively

Unlike the Sm-Nd data, the Rb-Sr isotope data do not fall on an isochron. The plagioclase-whole rock pair of sample UB19, however, yield an age of 1137 ± 50 Ma. Initial $^{87}\text{Sr}/^{86}\text{Sr}$ ratios calculated assuming the ~ 1500 Ma Sm-Nd mineral isochron age lie between 0.7032 and 0.7039 for the gabbroic rocks but are lower than 0.7 for the granites.

DISCUSSION

Emplacement age of the Rocks

Despite the large uncertainty, the whole rock Sm-Nd isochron ages show that, at the 95% confidence level, the gabbros and the granites were emplaced at the same time. The more precise mineral isochron age of 1505 ± 42 Ma obtained from one of the gabbros is therefore considered to date both the gabbroic and granitic magmatism.

The similarity in the emplacement ages of the two rock suites, coupled with the similarity in their initial $\epsilon(\text{Nd})$ values, support the interpretation of Stockley (1948) that the gabbroic and granitic rocks represent parallel differentiation trends from a common magma source. This interpretation is consistent with the observation that the two rock suites define a smooth trend that mimics the alkaline differentiation trend of Miyashiro (1974) on a total alkali ($\text{Na}_2\text{O} + \text{K}_2\text{O}$) versus SiO_2 diagram (Fig. 2). A co-genetic origin is also consistent with the fact that both suites appear to have formed by melting of a relatively deep source in which garnet was a residue phase as revealed by the LREE enriched and nearly flat HREE patterns of both suites.

The calculated $^{87}\text{Sr}/^{86}\text{Sr}$ initial ratios for the granitoids are < 0.7 suggesting that the rocks suffered post-emplacement addition of Rb most likely during the hydrothermal alteration event reflected in the strong sericitisation of their feldspars. This sericitisation is most intense close to shear zones associated with the Ukingan tectonism and is therefore likely to be a result of an Ukingan overprint on the rocks. Although the gabbro sample UB19 shows no sericitisation, its plagioclase-whole rock Rb-Sr age of 1137 ± 50 is best interpreted as dating the Ukingan overprint on the magmatic rocks.

Source characteristics

The ~ 1500 Ma emplacement age for the Msanyo-Mdando rocks is significantly older than the calculated T_{DM} ages of ~ 1700 to 1900 Ma. This suggests that the parental magma from which the rocks crystallised has been considerably contaminated by older crustal material. The gabbroic rocks, however, yield low $^{87}\text{Sr}/^{86}\text{Sr}$ initial ratios (0.7032 and 0.7039) indicating that the contaminant must have had a low Rb/Sr ratio. Such low ratios preclude contamination by upper continental crustal material. Contamination by lower crustal material can, however, account for both the near zero $\epsilon(\text{Nd})$ values and the relatively low $^{87}\text{Sr}/^{86}\text{Sr}$ ratios.

CONCLUSION

Isotopic and geochemical data suggest that the gabbros and granitoids in the Liganga-Msanyo-Mdando area crystallized from cogenetic mantle-derived melts which were emplaced in high grade metamorphic rocks of the Ubendian Belt at ~ 1500 Ma. The parental magma assimilated lower crustal material leading to an enriched Nd isotopic signature as reflected in the near zero $\epsilon(\text{Nd})$ values but preserving low $^{87}\text{Sr}/^{86}\text{Sr}$ initial ratios. The complex was subsequently sheared and sericitised locally during the Ukingan tectonism which is dated by a plagioclase-whole rock Rb-Sr age of ~ 1140 Ma.

ACKNOWLEDGEMENT

The support and friendship of Eizo Nakamura is greatly acknowledged. Chie Sakaguchi, Nobuko Takeuchi, Ryoji Tanaka, Hiroyuki Takei, Katsura Kobayashi and Akio Makishima offered valuable technical assistance during different stages of the experimental work. The research was conducted while the author was a Visiting Research Scholar at the Institute for the Study of the Earth's Interior, Okayama University at Misasa, Japan. Fieldwork was funded by a grant from the Sida/SAREC Core Support Facility to the Faculty of Science, University of Dar es Salaam.

REFERENCES

- Boynton WV 1984 Cosmochemistry of the rare earth elements: Meteorite studies. In: Henderson P (ed) *Rare earth element geochemistry*. Elsevier, Amsterdam, 63-107
- Brownlow AH 1996 *Geochemistry*. Prentice Hall, New Jersey
- Haldemann EG 1961 *QDS 274 – Milo*. Geological Survey of Tanganyika
- Ludwig KR 1994 Isoplot – a plotting and regression program for radiogenic isotope data. *US Geological Survey Open File Report*: 91-445
- MabokoMAH and Nakamura E 1996 Nd and Sr isotopic mapping of the Archean-Proterozoic boundary in southeastern Tanzania using granites as probes for crustal growth. *Precambrian Research* 77: 105-115
- Makishima A and Nakamura E 1997 Suppression of matrix effects in ICP-MS by high power operation of ICP: Application to precise determination of Rb, Sr, Y, Cs, Ba, REE, Pb, Th and U at ngg-1 levels in milligram silicate samples. *Geostandards Newsletter* 21: 307-319
- Michard A, Gurriet P, Soudant M and Albarede F 1985 Nd isotopes in French Phanerozoic shales: external vs internal aspects of crustal evolution. *Geochimica Cosmochimica et Acta* 49: 601-610
- Miyashiro A 1974 Volcanic rock series in island arc and active continental margins. *American Journal of Science* 274: 321-355
- Shibata T, Makishima A and Nakamura E 1989 *Trace neodymium isotope analysis and its appreciation to geological problems*. Paper presented at the 1989 Annual Meeting of the Geochemical Society of Japan, Tokyo, 73
- Stockley CM 1948 *Geology of North, West and Central Njombe District, Southern Highlands Province*. Witherby and Company Ltd., London
- Yoshikawa M and Nakamura E 1993 Precise isotopic determination of trace amounts of Sr in magnesium-rich samples. *Journal of the Japan Society for Mineralogy, Petrology and Economic Geology* 88: 548-561

